

Hard Thermal Photon Production in Relativistic Heavy Ion Collisions

Frank D. Steffen^{1,a} and Markus H. Thoma^{2,b,c}

¹*Institut für Theoretische Physik, Universität Heidelberg,
Philosophenweg 16, 69120 Heidelberg, Germany*

²*Theory Division, CERN, CH-1211 Geneva 23, Switzerland*

Abstract

The recent status of hard thermal photon production in relativistic heavy ion collisions is reviewed and the current rates are presented with emphasis on corrected bremsstrahlung processes in the quark-gluon plasma (QGP) and quark-hadron duality. Employing Bjorken hydrodynamics with an EOS supporting the phase transition from QGP to hot hadron gas (HHG), thermal photon spectra are computed. For SPS 158 GeV Pb+Pb collisions, comparison with other theoretical results and the WA98 direct photon data indicates significant contributions due to prompt photons. Extrapolating the presented approach to RHIC and LHC experiments, predictions of the thermal photon spectrum show a QGP outshining the HHG in the high- p_T -region.

Keywords: Bremsstrahlung, Quark-Gluon Plasma, Quark-Hadron Duality, Relativistic Heavy-Ion Collisions, Thermal Photon Production

PACS numbers: 12.38.Mh, 24.10.Nz, 24.85.+p, 25.75.-q

^aFrank.D.Steffen@thphys.uni-heidelberg.de

^bMarkus.Thoma@cern.ch

^cHeisenberg fellow

1 Introduction

Hard real photons are, as dileptons, promising for providing a signature of a quark-gluon plasma (QGP) possibly produced in relativistic heavy-ion collisions [1]. Direct photon spectra have been measured by the WA80 (upper limit) and the WA98 collaboration at the SPS [2, 3] and further data is expected from the RHIC and LHC heavy-ion experiments [4, 5]. For theoretical investigations on the SPS direct photon data and on RHIC and LHC predictions, prompt and thermal photon production rates must be convoluted with the space-time evolution of the fireball, while photons from the decay of hadrons after freeze-out are already subtracted in the experimental analysis.

In this work, the present status of hard thermal photon production in a QGP and a hot hadron gas (HHG) is reviewed critically. Contributions from the QGP are presented with emphasis on bremsstrahlung processes that are illustrated for the first time in their corrected form. Next, the photon producing processes in the HHG are discussed and a conservative estimate of the thermal rate is given. The review of the rates is completed by addressing the question of quark-hadron duality. With the obtained insights, the recent estimates of the rates are employed together with the well-understood Bjorken hydrodynamics [6, 7] to extract the essential features of the thermal and prompt photon yield in the phase transition scenario [8]. Comparison with other theoretical work demonstrates the competence of the simple hydrodynamical model at SPS energies and substantiates subsequent inspections of the WA98 data on direct photon production in SPS 158 GeV Pb+Pb collisions. For RHIC and LHC experiments, the rate estimations with the same hydrodynamical model are used to predict the p_T -range in which the QGP outshines the HHG.

2 Thermal Photon Production in the QGP

The production rate for hard ($E \gg T$) thermal photons¹ from an equilibrated QGP has been calculated in perturbative thermal QCD applying the hard thermal loop (HTL) resummation [10] to account for medium effects. The *Compton scattering* and *$q\bar{q}$ -annihilation* contribution

$$E \frac{dN}{d^4x d^3p} \Big|_{1-loop} = 0.0281 \alpha \alpha_s \ln \left(\frac{0.23 E}{\alpha_s T} \right) T^2 e^{-E/T}, \quad (1)$$

¹In the experimentally interesting case $E \gg T$ analytic expressions can be derived since e.g. Boltzmann distributions can be used for the outgoing partons [9].

is derived from the 1-loop HTL photon-polarisation tensor [9, 11, 12], while the contributions from *bremstrahlung*,

$$E \frac{dN}{d^4x d^3p} \Big|_{bremss} = 0.0219 \alpha \alpha_s T^2 e^{-E/T}, \quad (2)$$

and *q \bar{q} -annihilation with an additional scattering in the medium*,

$$E \frac{dN}{d^4x d^3p} \Big|_{q\bar{q}-aws} = 0.0105 \alpha \alpha_s E T e^{-E/T}, \quad (3)$$

are obtained from the 2-loop HTL photon-polarisation tensor [13], where all three rates are listed for a two-flavored ($N_f = 2$) QGP. Surprisingly, the 2-loop rates, (2) and (3), show up at order $\alpha \alpha_s$ and enhance the spectrum from the QGP phase by about a factor of 3 in the experimentally relevant p_T -range. Since earlier investigations on the importance of *bremstrahlung* processes in the QGP [14, 15, 16] employed the rates (2) and (3) multiplied *erroneously* by a factor of 4, we present this behavior for the first time in its corrected form.² The enhancement is anticipated by comparing the rates for fixed temperatures as shown in Fig. 1 and is documented in Fig. 2, where the thermal photon spectrum from the QGP, calculated in the model discussed below, is presented.³ Traced back to strong collinear singularities [13], this 2-loop enhancement substantially increased the interest in higher loop contributions. In fact, for real photons the 3-loop contribution turns out to be of the same order in α_s as the 2-loop contribution [18]. Since this is very likely the case for higher loop contributions as well, one can conclude that thermal photon production in the QGP is a non-perturbative mechanism that cannot be accessed in perturbative HTL resummed thermal field theory. Interestingly, ascribing the quarks a finite mean free path in the QGP, which simulates the Landau-Pomeranchuk-Migdal (LPM) effect, does not eliminate important non-perturbative aspects but helps to disarm the collinear singularities [19]. This points at possible destructive interferences via the LPM effect that do not allow one to interpret the sum of the rates (1), (2), and (3) as a lower limit. Adding further uncertainties such as the $g \ll 1$ assumption in the HTL calculations contrasted with realistic values of the strong coupling, $g = 2 - 3$, one must consider the sum of the rates (1), (2), and (3) only an educated guess. However, it is employed in this work as the best result available. Extensions to a QGP not in chemical equilibrium, which seems realistic at RHIC and LHC, can also be found [20, 21, 22, 23, 24].

²Due to a miscalculation of the two N_f -dependent constants J_T and J_L (exactly a factor 4 too large) in [13, 14], the derivation of the rates led to Eqs. (2) and (3) both multiplied by a factor of 4. In this way, an *erroneous* enhancement of the spectrum from the QGP phase by about *one order of magnitude* was found in the experimentally relevant p_T -range [14, 15, 16].

³In the QGP rates, $\alpha_s(T) = \frac{6\pi}{(33-2N_f)\ln(8T/T_c)}$ [17] is applied, where the number of flavors present in the QGP is set to $N_f = 2$ and the transition temperature is set to $T_c = 170$ MeV.

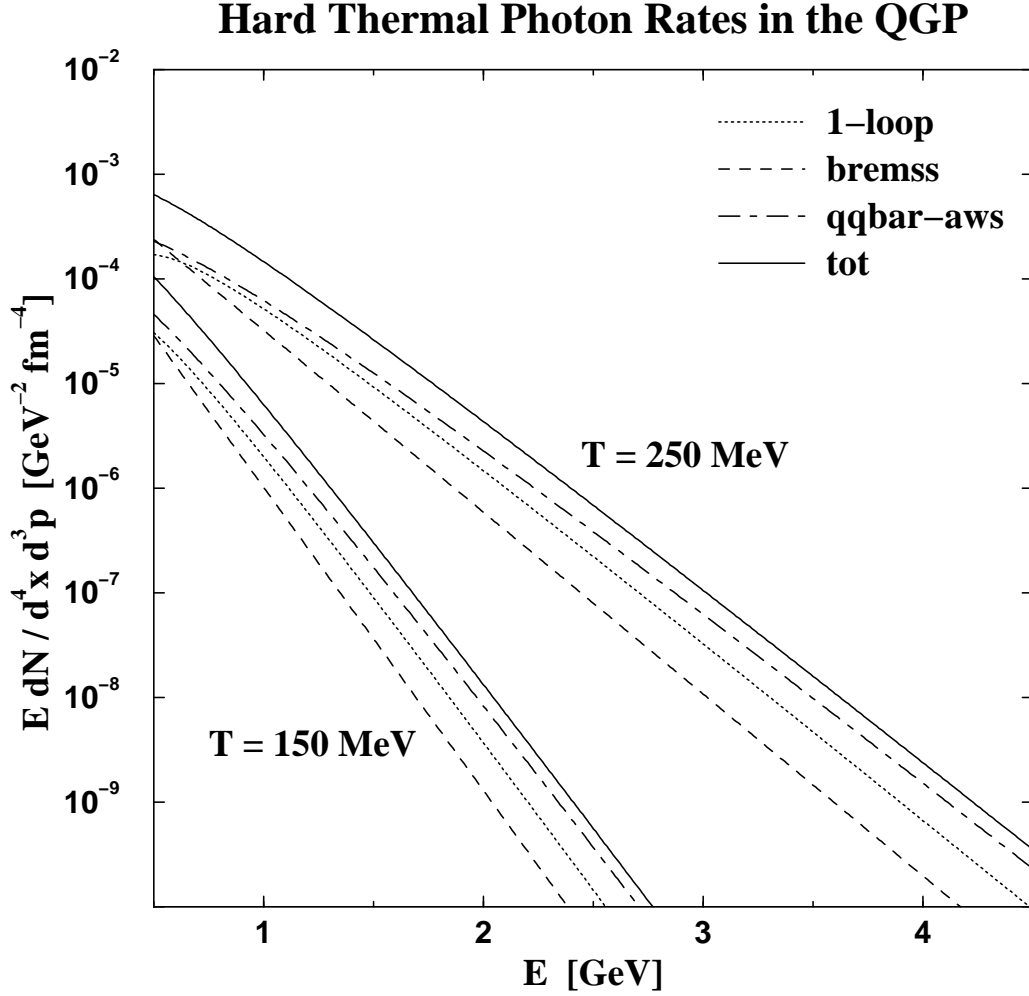


Figure 1: Hard Thermal Photon Rates in the QGP. For two fixed temperatures, $T = 150$ MeV (lower lines) and $T = 250$ MeV (upper lines), the QGP hard thermal photon rates (1), (2), and (3) are illustrated in the dotted, dashed and dot-dashed lines respectively, where the $\alpha_s(T)$ -parameterization of Karsch [17] is applied. The sum indicating the total QGP contribution up to 2-loop order is displayed in the solid lines. Inclusion of the 2-loop processes enhances the total QGP rate by about a factor of 3.

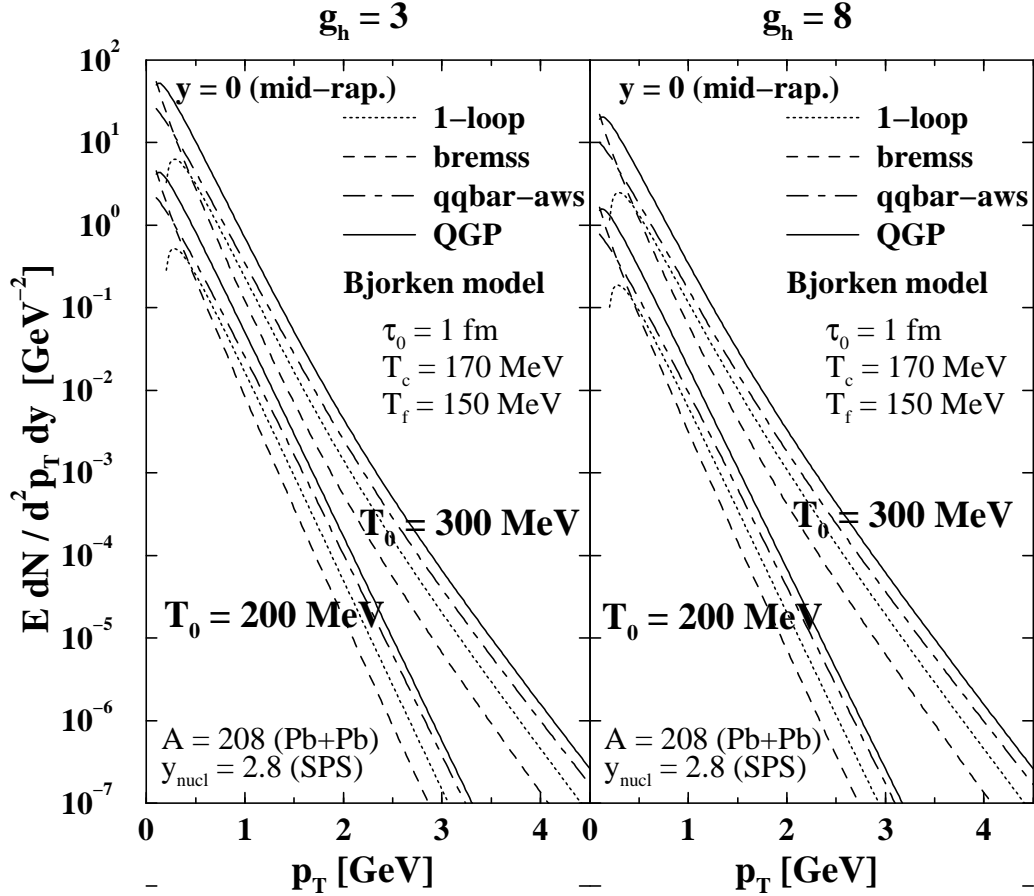


Figure 2: Hard Thermal Photon Spectrum from the QGP. The QGP contributions to the hard thermal photon yield from the rates (1), (2), (3), and the sum of these are illustrated in the dotted, dashed, dot-dashed and solid lines respectively. The integration of the rates over the space-time evolution of the fireball was performed in Bjorken hydrodynamics described in the text. Results are shown for two different initial temperatures, $T_0 = 200$ MeV (lower lines) and $T_0 = 300$ MeV (upper lines), and two different hadron gas EOS's characterized by $g_h = 3$ (left plot) and $g_h = 8$ (right plot) with the remaining parameters set to the displayed *typical* values. The 2-loop processes enhance the total QGP spectrum by about a factor of 3.

3 Thermal Photon Production in the HHG

The thermal photon production in an equilibrated hot hadron gas (HHG) is computed in effective theories with hadronic couplings inferred from experiment. A first investigation based on a model Lagrangian describing the interaction of π , ρ , and η mesons with photons found dominant contributions from the reactions $\pi\pi \rightarrow \rho\gamma$ and $\pi\rho \rightarrow \pi\gamma$ and from the decays $\omega \rightarrow \pi\gamma$ and $\rho \rightarrow \pi\pi\gamma$ [9, 25]. By considering additionally the $\pi\rho \rightarrow a_1 \rightarrow \pi\gamma$ reaction, a strong enhancement of the rate was observed [26]. This triggered a more complete and consistent computation using an effective chiral Lagrangian with π , ρ , and a_1 mesons. The result was an even higher rate due to the presence of the a_1 meson also in the $\pi\pi \rightarrow \rho\gamma$ and $\rho \rightarrow \pi\pi\gamma$ reactions [27, 28]. Keeping the strong dependence on the model Lagrangian and the uncertainties associated with medium effects in mind, the result parameterized in [28] supplemented by the $\omega \rightarrow \pi\gamma$ decay [9] can be considered as a *conservative* expression for the emissivity of the HHG. It is employed in this work using the formulas listed in the Appendix. For hard photons, $E > 1$ GeV, we found a rough estimate of this sum by multiplying the parameterization given in Eq. (18) of [26] by a factor of two

$$E \left. \frac{dN}{d^4x d^3p} \right|_{had} = 4.8 T^{2.15} e^{-1/(1.35 T E)^{0.77}} e^{-E/T}, \quad (4)$$

where photon energy E and temperature T are to be given in GeV to obtain the rate in units of $\text{fm}^{-4}\text{GeV}^{-2}$. Results from other Lagrangians can be found in [29, 30] and medium effects are investigated in [28, 30, 31, 32], where a significant increase of the static rate is observed by dropping the in-medium meson masses that is, however, in part compensated in the spectrum through a consequent modification of the fireball evolution. Further, the influence of finite chemical potential [31], finite baryon density [33] and additional reactions involving a_1 , b_1 , K_1 , and other strange mesons [34, 35] have been considered but are neglected in this work.

4 Quark-Hadron Duality

In order to test the hypothesis of quark-hadron duality in photon production [36, 37], we compare the discussed QGP and HHG hard thermal photon rates for two fixed temperatures, $T = 150$ and 200 MeV, as shown in Fig. 3, where the solid and dashed lines indicate the QGP and the HHG contributions respectively. For temperatures between 150 MeV and 200 MeV, an energy window can be found, where the steeper QGP and the flatter HHG emissivities cross. Considering the uncertainties in the rates, the validity of the classic statement 'the hadron gas shines

Thermal Photon Rates & Quark-Hadron Duality

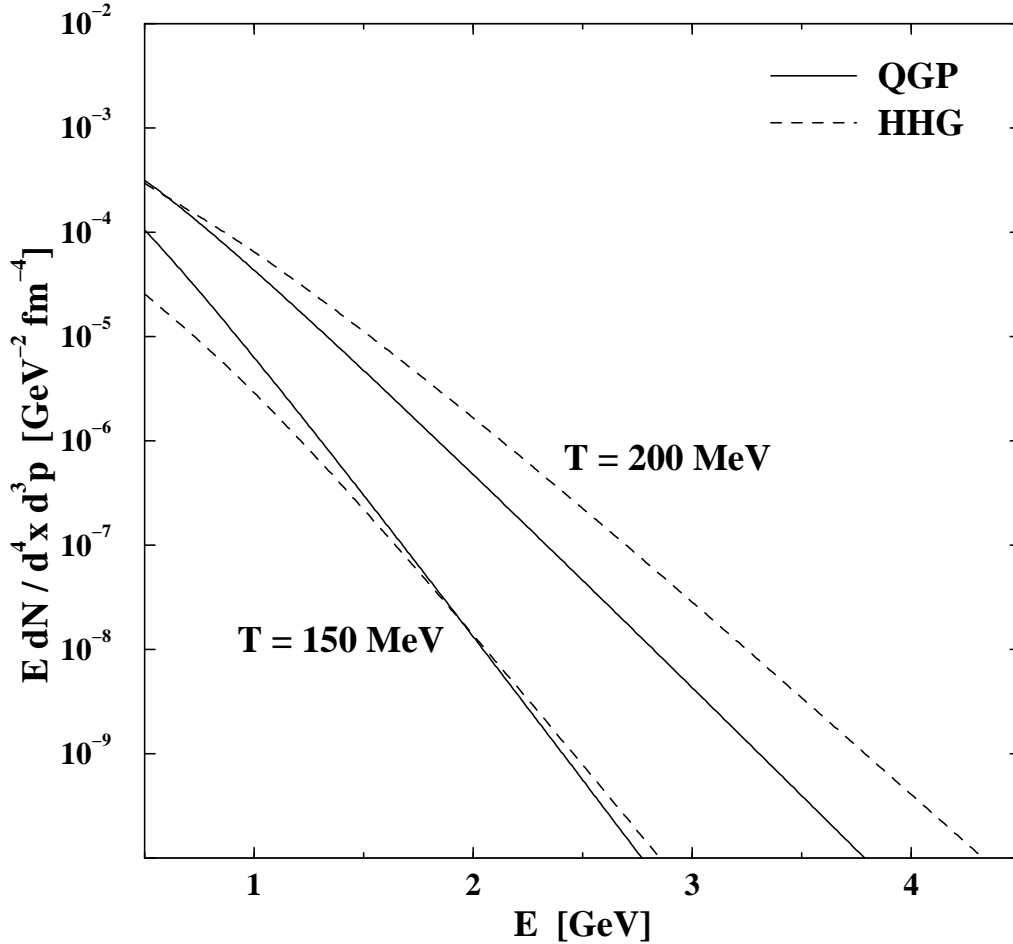


Figure 3: Quark-Hadron Duality in the Hard Thermal Photon Rates. The sum of the QGP contributions (1), (2), and (3), illustrated in the solid lines, and that of the HHG contributions (Song’s results [27, 28] supplemented by the $\omega \rightarrow \pi\gamma$ decay [9]), illustrated in the dashed lines, are compared for two fixed temperatures, $T = 150 \text{ MeV}$ (lower lines) and $T = 200 \text{ MeV}$ (upper lines), where the $\alpha_s(T)$ -parameterization of Karsch [17] is applied in the QGP rates. Considering the uncertainties in the rates, quark-hadron duality in the rates at a certain temperature can neither be confirmed nor be ruled out.

as brightly as the quark-gluon plasma' [9] can neither be confirmed nor be ruled out, at least in a certain temperature regime, by taking into account the 2-loop QGP processes and the a_1 meson in the HHG. However, as indicated by Fig. 3, there is no reason to assume that the photon production rates from the two phases coincide at all temperatures. But even if the rates of the two phases agree in the relevant temperature regime, the spectrum might be changed by the presence of the QGP due to a different space-time evolution.

5 Thermal Photon Spectrum

The observable quantity is the spectrum of direct photons which is calculated theoretically by convoluting the prompt and thermal photon rates with the space-time evolution of the fireball produced in heavy-ion collisions. Concentrating on the effects of the thermal photon rates, we describe the thermalized collision phase in Bjorken-1+1-hydrodynamics [6, 7] taking an EOS with a first-order phase transition from a QGP, modelled by a massless two-flavored parton gas, to a HHG, modelled by a massless pion gas. This well-understood, simple approach allows us to demonstrate very clearly the influences of the rates on the spectrum, and interestingly, comparison with other work shows it to be as competent as 2+1 hydrodynamical models at least at SPS energies [16]. This means that at SPS the transverse expansion has only minor effects on the photon production.

5.1 Comparison with other Work

The WA98 direct photon data analysis of Gallmeister et al. obtained in a model describing a *spherically* symmetric expansion [37] can be reproduced in the simple model with the discussed rates.⁴ By assuming a thermalization time of $\tau_0 = 1$ fm and equal initial, transition, and freeze-out temperatures of $T_0 = T_c = T_f = 170$ MeV as in [37], i.e. only a mixed phase, this single temperature value suffices to describe the WA98 data [2, 3] when the prompt photon estimation of [37] is added.

It is also possible to reproduce the WA98 direct photon data analysis of Srivastava et al. [39], which does not necessitate prompt photons but instead initial conditions that are rather extreme for SPS, i.e. a very small thermalization time of $\tau_0 = 0.2$ fm and a very high initial temperature of $T_0 = 335$ MeV. Since their analysis was performed using the 2-loop QGP rates by mistake multiplied by a factor of 4, even smaller thermalization times together with higher initial temperatures are demanded when applying the corrected 2-loop QGP rates. This is due to the

⁴The $\omega \rightarrow \pi\gamma$ decay is not taken into account since electromagnetic meson decays were subtracted in the experimental analysis of the WA98 collaboration [38].

relative importance of the QGP rates in the high p_T -range. Concentrating on a validity-check of the simple model, a comparison using *the same erroneous* rates is performed. While the QGP thermal photon spectrum obtained in our simple model matches directly the one of Srivastava et al. [39], we must increase the effective degrees of freedom in the ideal massless pion gas from the actual value of $g_h = 3$ to an effective one of $g_h = 8$ in order to achieve the fit in the HHG thermal photon spectrum. This points to the *rich* HHG EOS employed in [39] having a much stronger effect than transverse expansion.

5.2 Thermal Photon Spectrum from the QGP

These insights into the reliability of the simple model substantiate the QGP thermal photon spectrum calculated in this model and shown in Fig. 2 to illustrate the effect of 2-loop processes in the QGP. Displaying the spectrum not only for $g_h = 3$ (left plot) but also for $g_h = 8$ (right plot) demonstrates additionally the effect of a richer HHG EOS, which lowers the QGP thermal photon yield by reducing the lifetime of the mixed phase.

5.3 Comparison with WA98 Direct Photon Data

The total thermal photon spectrum emerging from the discussed rates in the simple model can be exploited by using the WA98 measurements of the direct photon yield [3] to specify upper limits on the initial temperature, T_0^{max} , reached in the SPS 158 GeV Pb+Pb collisions. This is presented in Fig. 4. For *typical* parameters $\tau_0 = 1$ fm, $T_c = 170$ MeV, $T_f = 150$ MeV, nucleon number $A = 208$ (corresponding to Pb + Pb collisions), projectile rapidity $y_{nucl} = 2.8$ (corresponding to a center-of-mass energy of $\sqrt{s} = 17$ GeV), and with an ideal massless pion gas of $g_h = 3$ effective degrees of freedom, even with an initial temperature of $T_0 = T_c = 170$ MeV (dotted line) the computed spectrum *exceeds* the experimental limits at low p_T ! Simulating the richer HHG EOS by setting $g_h = 8$, the lifetime of the mixed and pure HHG phase drops, resulting in a decrease of the spectrum that brings back the possibility of having a phase transition scenario with $T_0^{max} = 220$ MeV (short dashed line). By reducing the critical temperature to $T_c = 160$ MeV, the mean temperature is reduced enabling also for $g_h = 3$ the phase transition scenario with $T_0^{max} = 175$ MeV (solid line). For $g_h = 8$ and $T_c = 160$ MeV, $T_0^{max} = 235$ MeV (long dashed line) is found, which might be interpreted as an upper bound on the initial temperature reached in the SPS 158 GeV Pb+Pb collisions.⁵ However, the

⁵Due to the mentioned possible destructive interferences via the LPM effect in the QGP, the presented T_0^{max} values cannot represent *rigid* upper bounds. They rather indicate the magnitude and point to the *relative* differences caused by different model scenarios.

WA98 Direct Photon Data & Thermal Spectrum

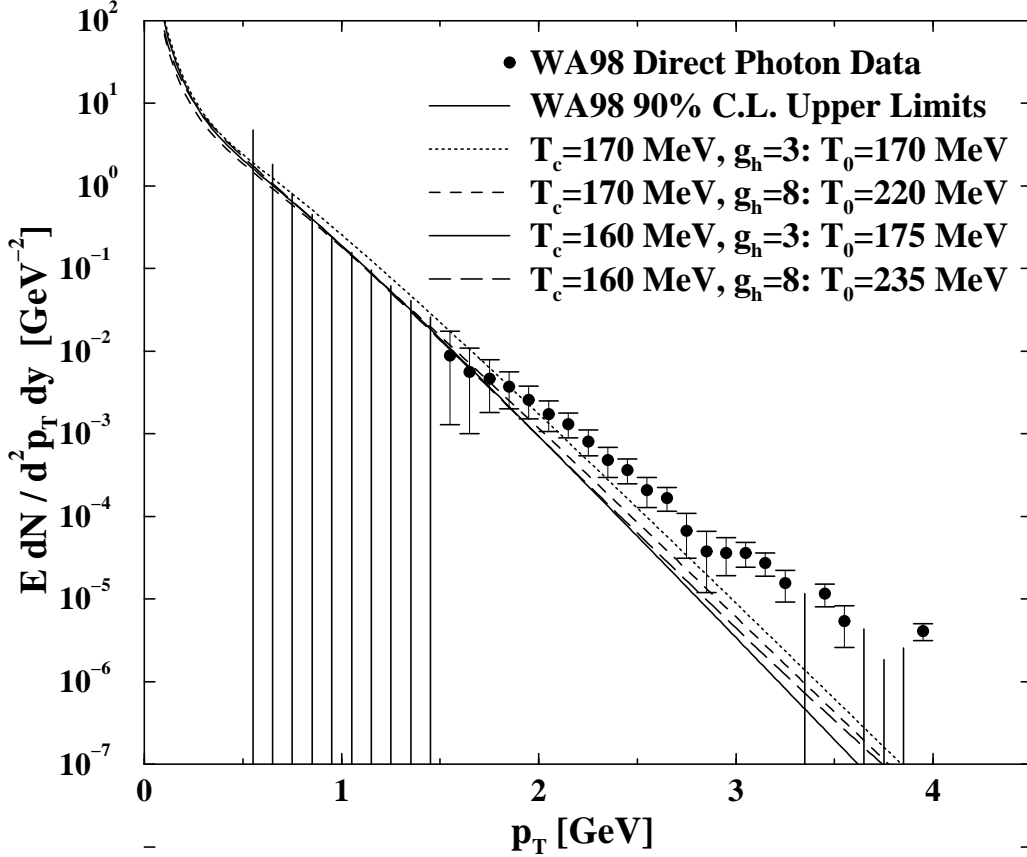


Figure 4: WA98 Direct Photon Data and Upper Limits on the Initial Temperature. The theoretical spectra supporting the phase transition from QGP to HHG (solid, short-dashed, and long-dashed lines) are compared with the experimental upper limits (vertical lines) and data (points with error bars). The discrepancy in the high- p_T -region demonstrates that a significant prompt photon contribution is necessary for a theoretical explanation of the experimental results within the phase transition scenario.

Accelerator / Collider	Experiment	A	\sqrt{s} [A·GeV]	y_{nucl}	dN/dy	τ_0 [fm]	T_0 [MeV]
SPS	WA98	208	17	2.8	825	1.0	190
RHIC	PHENIX	208	200	5.3	1734	0.5	310
LHC	ALICE	208	5500	8.6	5625	0.5	450

Table 1: Parameters used in the Predictions of the Thermal Photon Spectrum for RHIC and LHC Experiments. The listed values for multiplicity dN/dy , thermalization time τ_0 , and initial temperature T_0 are the estimates given in [14].

spectra supporting the phase transition from QGP to HHG cannot describe the direct photon data for $p_T > 2$ GeV as shown in Fig. 4. This discrepancy in the high- p_T -region demonstrates that a significant prompt photon contribution is necessary for a theoretical explanation of the experimental results within the phase transition scenario.

5.4 Predictions for RHIC and LHC

Finally, we employ the simple model to extract predictions for RHIC and LHC. Although earlier comparisons with [14] revealed a more important transverse expansion [16], it is interesting to locate in the above approach the p_T -range in which the QGP outshines the HHG. Assuming a three-flavored QGP, the prefactors on the rhs in Eqs. (1), (2), and (3) become 0.0338, 0.0281, and 0.0135 respectively. Further, the SPS, RHIC, and LHC parameters of [14] are adopted as summarized in Tab. 1. Figure 5 shows our results for the QGP, HHG, and sum of both contributions in the dashed, dotted, and solid lines respectively. The spectra for $g_h = 3$ are shown on the left and the ones for $g_h = 8$ on the right. As a reference point, the SPS result obtained with the parameters of [14] is also presented. For $g_h = 3$ ($g_h = 8$), the QGP outshines the HHG for $p_T > 3.2$ GeV ($p_T > 2.2$ GeV) at RHIC and for $p_T > 2.5$ GeV ($p_T > 1.7$ GeV) at LHC, while at SPS photons from HHG dominate the spectrum for $g_h = 3$ and $g_h = 8$ at all p_T 's. Since the employed simple model does not describe deviations from chemical equilibrium, the reader is referred to [24], where this issue is addressed systematically and RHIC and LHC predictions are provided for the QGP photon emissivity.

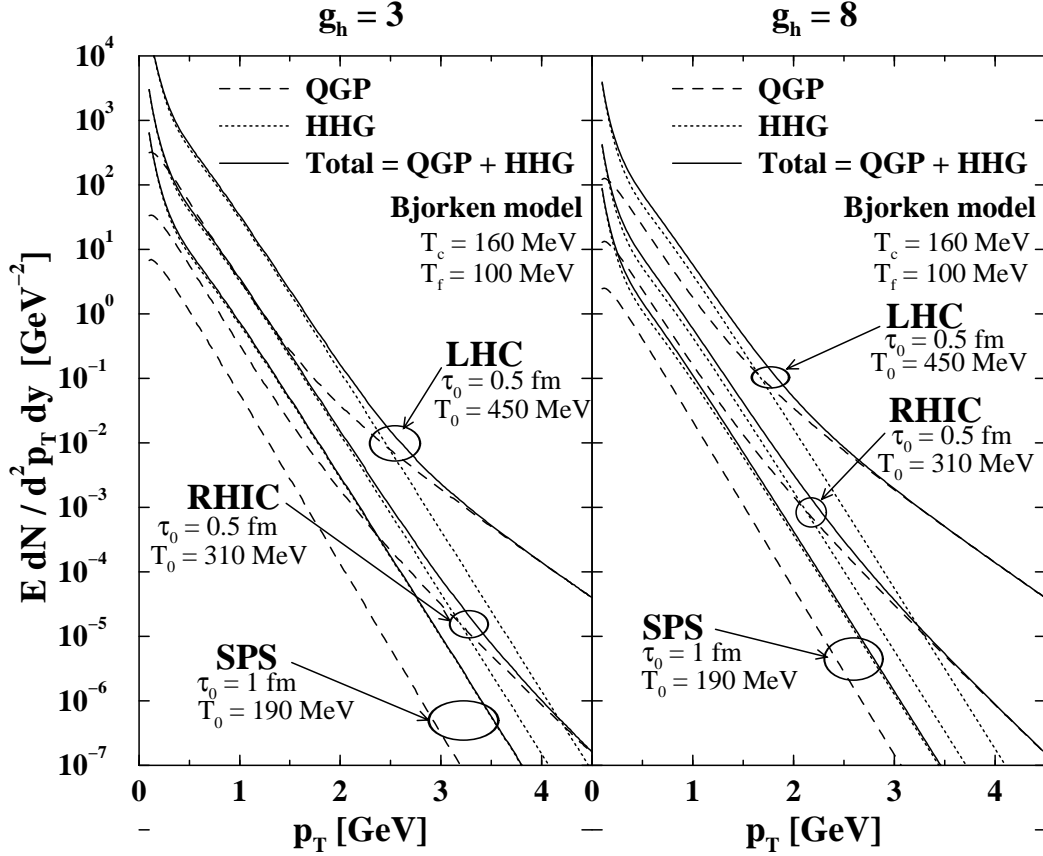


Figure 5: QGP vs. HHG Photon Emissivities in SPS, RHIC, and LHC Pb+Pb Collisions. For $g_h = 3$ ($g_h = 8$), the QGP outshines the HHG for $p_T > 3.2 \text{ GeV}$ ($p_T > 2.2 \text{ GeV}$) at RHIC and for $p_T > 2.5 \text{ GeV}$ ($p_T > 1.7 \text{ GeV}$) at LHC, while at SPS photons from HHG dominate the spectrum for $g_h = 3$ and $g_h = 8$ at all p_T 's. The initial conditions vary from ($\tau_0 = 1 \text{ fm}$, $T_0 = 190 \text{ MeV}$) at SPS over ($\tau_0 = 0.5 \text{ fm}$, $T_0 = 310 \text{ MeV}$) at RHIC to ($\tau_0 = 0.5 \text{ fm}$, $T_0 = 450 \text{ MeV}$) at LHC, while the same values of $T_c = 160 \text{ MeV}$ and $T_f = 100 \text{ MeV}$ are chosen.

6 Conclusion

We have discussed the hard thermal photon production in relativistic heavy ion collisions using the most recent estimates for the photon production rates from the QGP and the HHG. For the first time, the enhancement of the QGP thermal photon rate and yield due to bremsstrahlung processes was presented in its corrected form. The consideration of these processes hinted at the recently confirmed non-perturbative nature of thermal photon production in the QGP [18]. The derivation of a reliable rate requires now new developments in thermal field theory [19]. For thermal photon production in the HHG, the strong dependence on assumptions regarding the thermalized hadron species, their interactions, and the role of medium effects was emphasized. We identified the best estimates available for the QGP and HHG rates and presented a convenient parameterization for the total HHG rate. Using these estimates, we could find no indication of a quark-hadron duality in the photon production rate.

Integrating the rate estimations over the space-time evolution of the fireball modelled in Bjorken hydrodynamics, we obtained the thermal photon spectrum. Comparison with other models, which describe transverse expansion of the fireball, demonstrated the competence of the simple model for the phase transition scenario at SPS energies and substantiated the subsequent investigation of the WA98 direct photon data. We found that this experimental data allows no conclusion to be drawn about the existence of a QGP phase at SPS but can be explained by a conservative thermal source *plus* prompt photons. Finally, the simple model was employed also for RHIC and LHC energies and predicted a QGP outshining the HHG in the high- p_T -range. If this picture is not spoiled by transverse expansion and chemical non-equilibrium or covered by dominant prompt photon contributions, the RHIC and LHC experiments might see thermal photons from the QGP in a certain photon momentum range that could provide the desired signature of the QGP.

As RHIC is already taking data and LHC under construction, a reliable expression for the thermal photon production rate in the QGP is of utmost importance. Optimistically the final result could reveal photons to be a smoking gun for the production of the QGP. In order to reduce the uncertainties concerning the fireball evolution, we recommend a combined investigation of real photon, dilepton, and hadron spectra, similar to the one of Sollfrank et al. [40], in which aspects such as different EOS's, finite baryon density, chemical non-equilibrium, and transverse expansion should be addressed in a systematic way. Once such an investigation is completed in accordance with the SPS data, it should be extended to RHIC and LHC energies to obtain serious predictions.

Acknowledgements

We thank Munshi Mustafa for helpful and interesting discussions.

Appendix

The employed rate for thermal photon production in the HHG is composed of the exact expression for the decay $\omega \rightarrow \pi\gamma$ [9] and the parameterizations for the processes $\pi\pi \rightarrow \rho\gamma$, $\pi\rho \rightarrow \pi\gamma$, and $\rho \rightarrow \pi\pi\gamma$, in which the a_1 meson is taken into account properly [27, 28]. For completeness and convenience, the explicit formulas are listed. By inserting E , T , and the pion mass m_π in GeV, the following parameterizations for $process = \pi\pi \rightarrow \rho\gamma$, $\pi\rho \rightarrow \pi\gamma$, and $\rho \rightarrow \pi\pi\gamma$ reproduce the corresponding rates in units of $\text{fm}^{-4}\text{GeV}^{-2}$ [28]

$$E \frac{dN}{d^4x d^3p} \Big|_{process} = T^2 e^{-E/T} F_{process}(T/m_\pi, E/m_\pi), \quad (5)$$

where

$$F_{\pi\pi \rightarrow \rho\gamma}(x, y) = \exp[-12.055 + 4.387x + (0.3755 + 0.00826x)y + (-0.00777 + 0.000279x)y^2 + (5.7869 - 1.0258x)/y + (-1.979 + 0.58x)/y^2], \quad (6)$$

$$F_{\pi\rho \rightarrow \pi\gamma}(x, y) = \exp[-2.447 + 0.796x + (0.0338 + 0.0528x)y + (-21.447 + 8.2179x)/y + (1.52436 - 0.38562x)/y^2], \quad (7)$$

$$F_{\rho \rightarrow \pi\pi\gamma}(x, y) = \exp[-6.295 + 1.6459x + (-0.4015 + 0.089x)y + (-0.954 + 2.05777x)/y]. \quad (8)$$

No parameterization is used for the decay of the ω meson since the exact expression requires only a one-dimensional integration [9]

$$E \frac{dN}{d^4x d^3p} \Big|_{\omega \rightarrow \pi\gamma} = \frac{8.93 \times 10^{-6} \text{ GeV}}{E} \int_{E_{min}}^{\infty} dE_\omega E_\omega f_B(E_\omega) [1 + f_B(E_\omega - E)], \quad (9)$$

where $E_{min} = 1.03 (E^2 + 0.14 \text{ GeV}^2)/E$ and $f_B(E) = 1/[\exp(E/T) - 1]$.

References

- [1] P.V. Ruuskanen, Nucl. Phys. **A544** (1992) 169c.
- [2] WA80 Collab., R. Albrecht et al., Phys. Rev. Lett. **76** (1996) 3506.
- [3] WA98 Collab., M.M. Aggarwal et al., nucl-ex/0006007 (2000).
- [4] D.P. Morrison (PHENIX Collab.), Nucl. Phys. **A638** (1998) 565c.
- [5] ALICE Collab., Technical Proposal, CERN/LHCC 95-71; Addendum to Technical Proposal, CERN/LHCC 96-32; C. Lourenco (ALICE Collab.), hep-ph/9612221 (1996).
- [6] J.D. Bjorken, Phys. Rev. **D27** (1983) 140.
- [7] M. Gyulassy and T. Matsui, Phys. Rev. **D29** (1984) 419.
- [8] H. Satz, Z. Phys. **C62** (1994) 683.
- [9] J. Kapusta, P. Lichard, and D. Seibert, Phys. Rev. **D44** (1991) 2774; **D47** (1993) 4171.
- [10] E. Braaten and R.D. Pisarski, Nucl. Phys. **B337** (1990) 569.
- [11] R. Baier, H. Nakkagawa, A. Niégawa, and K. Redlich, Z. Phys. **C53** (1992) 433.
- [12] C.T. Traxler, H. Vija, and M.H. Thoma, Phys. Lett. **B346** (1995) 329.
- [13] P. Aurenche, F. Gelis, R. Kobes, and H. Zaraket, Phys. Rev. **D58** (1998) 085003; hep-ph/9804224. Note that the numerical two-flavor values for J_T and J_L , given in Sec. 4.4, are exactly a factor 4 too large due to an error in the employed computer program.
- [14] D.K. Srivastava, Eur. Phys. J. **C10** (1999) 487; nucl-th/9904010. Note that the numerical two- and three-flavor values for J_T and J_L , given between Eqs. (2) and (3), are incorrect, i.e. as in [13] exactly a factor 4 too large.
- [15] D.K. Srivastava and B.C. Sinha, Eur. Phys. J. **C12** (2000) 109.
- [16] F.D. Steffen, Bremsstrahlung out of the Quark-Gluon Plasma, Diplomarbeit, Universität Giessen (1999); nucl-th/9909035.
- [17] F. Karsch, Z. Phys. **C38** (1988) 147.
- [18] P. Aurenche, F. Gelis, and H. Zaraket, Phys. Rev. **D61** (2000) 116001.
- [19] P. Aurenche, F. Gelis, and H. Zaraket, Phys. Rev. **D62** (2000) 096012.

- [20] M. Strickland, Phys. Lett. **B331** (1994) 245.
- [21] C.T. Traxler and M.H. Thoma, Phys. Rev. **C53** (1996) 1348.
- [22] D.K. Srivastava, M.G. Mustafa, and B. Müller, Phys. Rev. **C56** (1997) 1064.
- [23] R. Baier et al., Phys. Rev. **D56** (1997) 2548.
- [24] M.G. Mustafa, M.H. Thoma, Phys. Rev. **C62** (2000) 014902.
- [25] H. Nadeau, J. Kapusta, and P. Lichard, Phys. Rev. **C45** (1992) 3034; **C47** (1993) 2426.
- [26] L. Xiong, E. Shuryak, and G.E. Brown, Phys. Rev. **D46** (1992) 3798.
- [27] C. Song, Phys. Rev. **C47** (1993) 2861.
- [28] C. Song and G. Fai, Phys. Rev. **C58** (1998) 1689.
- [29] J.K. Kim, P. Ko, K.Y. Lee, and S. Rudaz, Phys. Rev. **D53** (1996) 4787.
- [30] M.A. Halász, J.v. Steele, G. Li, and G.E. Brown, Phys. Rev. **C58** (1998) 365.
- [31] J.V. Steele, H. Yamagishi, and I. Zahed, Phys. Lett. **B384** (1996) 255.
- [32] S. Sarkar et al., Nucl. Phys. **A634** (1998) 206.
- [33] J.V. Steele, H. Yamagishi, and I. Zahed, Phys. Rev. **D56** (1997) 5605.
- [34] K. Haglin, Phys. Rev. **C50** (1994) 1688.
- [35] C.-H. Lee, H. Yamagishi, and I. Zahed, Phys. Rev. **C58** (1998) 2899.
- [36] R. Rapp and J. Wambach, hep-ph/9909229 (1999).
- [37] K. Gallmeister, B. Kämpfer, and O.P. Pavlenko, hep-ph/0006134 (2000).
- [38] T. Peitzmann (WA98 Collab.), private communication.
- [39] D.K. Srivastava and B. Sinha, nucl-th/0006018 (2000).
- [40] J. Sollfrank et al., Phys. Rev. **C55** (1997) 392.

**Erratum to: “Hard Thermal Photon Production
in Relativistic Heavy Ion Collisions”
[Phys. Lett. B 510 (2001) 98]**

Frank D. Steffen^{1,a} and Markus H. Thoma^{2,b}

¹*Max-Planck-Institut für Physik (Werner Heisenberg Institut)
Föhringer Ring 6, D-80805 Munich, Germany*

²*Max-Planck-Institut für extraterrestrische Physik
P.O. Box 1312, D-85741 Garching, Germany*

In the original paper [1] the ordinates of Figs. 2, 4, and 5 are labeled incorrectly. For all three figures, the correct label reads $dN/d^2p_T dy$ [GeV⁻²]. The figures with the correct labels are given below with numberings and captions adopted from the original paper [1].

Acknowledgements

We thank Serguei Kiselev for pointing out the error in the labels.

References

- [1] F. D. Steffen and M. H. Thoma, Phys. Lett. B **510** (2001) 98 [arXiv:hep-ph/0103044].

^asteffen@mppmu.mpg.de

^bthoma@mpe.mpg.de

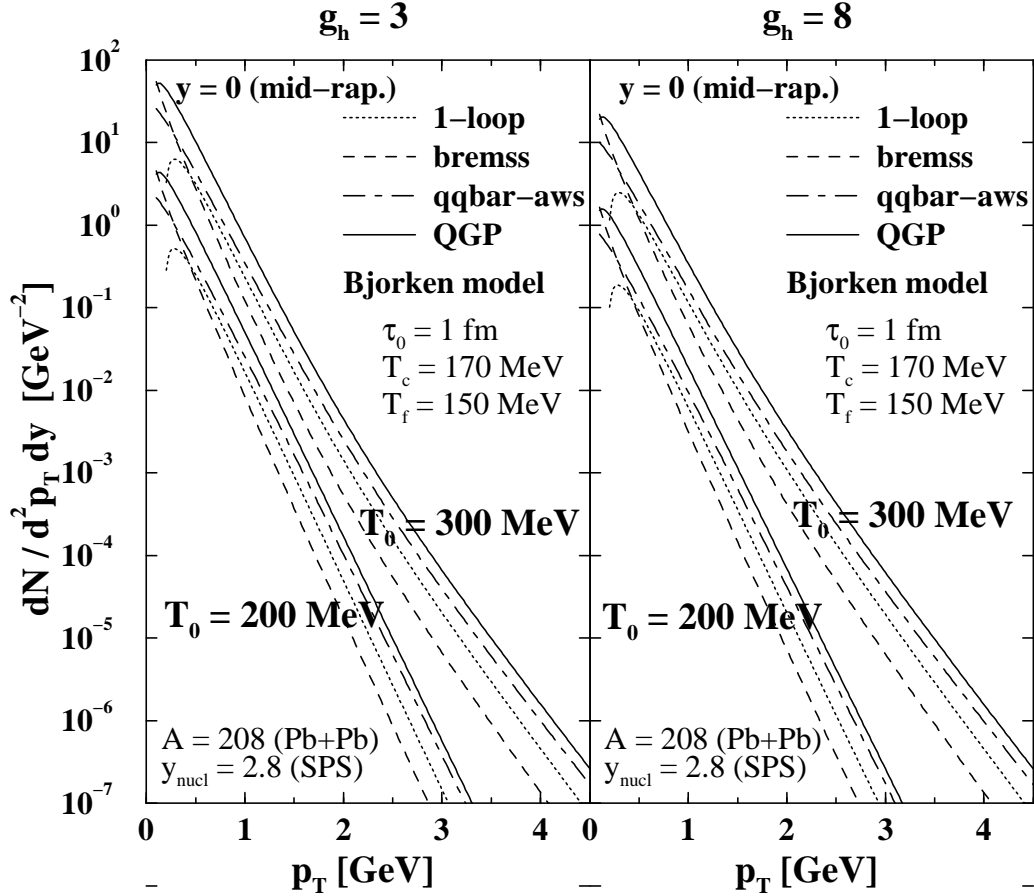


Figure 2: Hard Thermal Photon Spectrum from the QGP. The QGP contributions to the hard thermal photon yield from the rates (1), (2), (3), and the sum of these are illustrated in the dotted, dashed, dot-dashed and solid lines respectively. The integration of the rates over the space-time evolution of the fireball was performed in Bjorken hydrodynamics described in the text. Results are shown for two different initial temperatures, $T_0 = 200$ MeV (lower lines) and $T_0 = 300$ MeV (upper lines), and two different hadron gas EOS's characterized by $g_h = 3$ (left plot) and $g_h = 8$ (right plot) with the remaining parameters set to the displayed *typical* values. The 2-loop processes enhance the total QGP spectrum by about a factor of 3.

WA98 Direct Photon Data & Thermal Spectrum

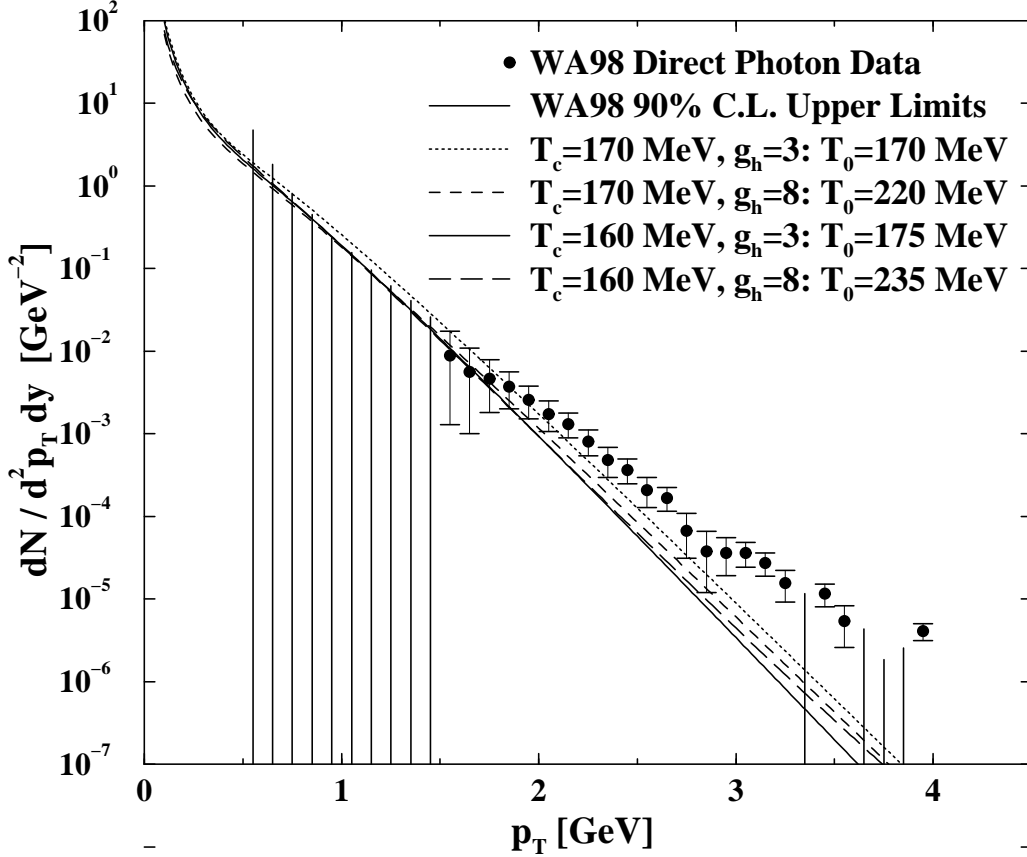


Figure 4: WA98 Direct Photon Data and Upper Limits on the Initial Temperature. The theoretical spectra supporting the phase transition from QGP to HHG (solid, short-dashed, and long-dashed lines) are compared with the experimental upper limits (vertical lines) and data (points with error bars). The discrepancy in the high- p_T -region demonstrates that a significant prompt photon contribution is necessary for a theoretical explanation of the experimental results within the phase transition scenario.

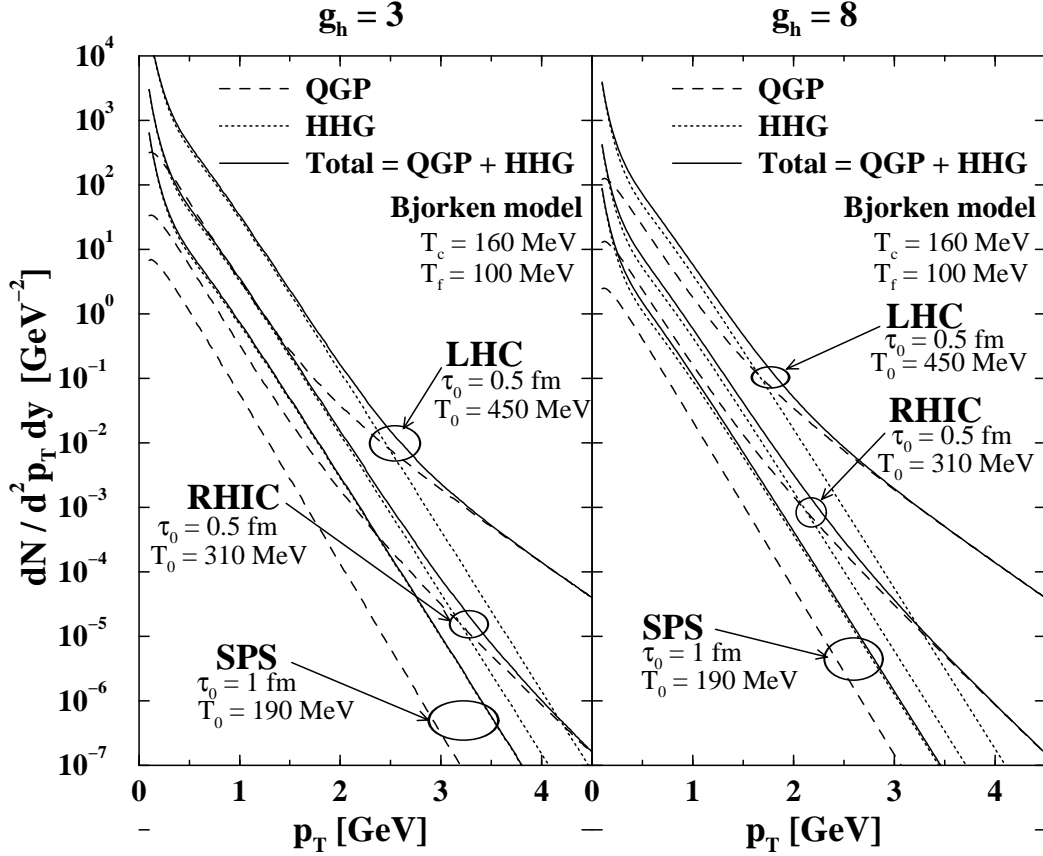


Figure 5: QGP vs. HHG Photon Emissivities in SPS, RHIC, and LHC Pb+Pb Collisions. For $g_h = 3$ ($g_h = 8$), the QGP outshines the HHG for $p_T > 3.2$ GeV ($p_T > 2.2$ GeV) at RHIC and for $p_T > 2.5$ GeV ($p_T > 1.7$ GeV) at LHC, while at SPS photons from HHG dominate the spectrum for $g_h = 3$ and $g_h = 8$ at all p_T 's. The initial conditions vary from ($\tau_0 = 1$ fm, $T_0 = 190$ MeV) at SPS over ($\tau_0 = 0.5$ fm, $T_0 = 310$ MeV) at RHIC to ($\tau_0 = 0.5$ fm, $T_0 = 450$ MeV) at LHC, while the same values of $T_c = 160$ MeV and $T_f = 100$ MeV are chosen.